EUROPEAN ORGANIZATION FOR NUCLEAR RESEARCH

Proposal to the ISOLDE and Neutron Time-of-Flight Committee

Penning-trap mass spectrometry of neutron-rich copper isotopes for probing the $Z = 28$ and $N = 50$ shell closures

January 4, 2012

V. Manea[1], D. Beck[2], K. Blaum[3], Ch. Böhm[3], Ch. Borgmann[3], M. Breitenfeldt[4], T. Eronen[3], F. Herfurth[2], M. Kowalska[5], S. Kreim[3,5], D. Lunney[1], S. Naimi[6], D. Neidherr[2], M. Rosenbusch[7], L. Schweikhard[7], J. Stanja[8], F. Wienholtz[7], R. N. Wolf[7], K. Zuber[8]

[1] CSNSM-IN2P3-CNRS, Université Paris-Sud 11, Orsay, France
[2] GSI Helmholtzzentrum für Schwerionenforschung GmbH, Darmstadt, Germany
[3] Max Planck Institute for Nuclear Physics, Heidelberg, Germany
[4] IKS Leuven, Belgium
[5] CERN, Geneva, Switzerland
[6] RIKEN Research Facility, Japan
[7] Ernst-Moritz-Arndt-University, Greifswald, Germany
[8] Technical University, Dresden, Germany

Spokesperson: Vladimir Manea (vladimir.manea@cern.ch)
Local contact: Susanne Kreim (skreim@cern.ch)

CERN-INTC-2012-004 / INTC-P-321
04/01/2012

Abstract

We propose to perform a Penning-trap mass measurement of ^{79}Cu. This exotic $N = 50$ isotone is the last frontier before the doubly-magic ^{78}Ni and will greatly improve our knowledge of shell evolution. In the same run, we propose $^{77-78}$Cu mass measurements, as well as the search for a possible isomer in ^{76m}Cu. The data will help to clarify the structure of the odd proton in the Cu isotopes, the influence on the $Z = 28$ proton core of the $vg_{9/2}$ orbital filling and the impact of the proton-neutron residual interaction on the strength of the $N = 50$ shell closure.

Requested shifts: We request 14 shifts in a single run, using a UC_x target and the resonant laser ionization of the Cu isotopes (RILIS). We also request use of the HRS and slits for suppressing Rb and Ga contaminants.

1. Introduction

The enhanced stability of nuclides having certain "magic" numbers of protons and neutrons (2, 8, 20, 28, 50, 82, 126) was the first striking experimental evidence that the simple liquid-drop picture of the atomic nucleus cannot account for the full complexity of its structure. This evidence suggested that nuclei might exhibit properties analogous to the atomic systems, pointing towards the existence of nuclear shells. The requirement of explaining the occurrence of magic numbers led to the formulation of the nuclear shell model and enforced the concept of mean-field at the nuclear level. It also offered the first experimental constraint on the form of the nuclear potential, since a strong spin-orbit coupling was postulated for the shell model to predict the correct magic numbers [1, 2].

The nuclear data provided by the modern radioactive ion-beam facilities have enlarged the experimental basis upon which the theoretical nuclear-structure approaches are developed, including the properties of nuclei farther and farther away from the region of stability of the nuclear chart. This newer experimental evidence constitutes a challenge, both for the shell-model picture of the nucleus and for the understanding of the nuclear potential. The typical experimental signatures for magicity, like the high empirical shell gaps [3], low $B(E2; 0^+ \rightarrow 2^+)$ values and 2^+ excited-state energies [4], become less pronounced for exotic magic nuclei. This, on the one hand, brings into question the universality of the shell-model picture of the nucleus and, on the other hand, hints towards new nuclear-structure features, such as the effects of the tensor component of the residual interaction, in the shell-model framework [4-6], and the importance of beyond mean-field correlations in the Density-Functional-Theory approaches, such as quadrupole correlations [7]. An important problem arising is tracing the origin of this evolution of the experimental observables to either a change in the single-particle energies or to enhanced collectivity in the nuclear many-body system [8]. If the changes are at the level of the single-particle energies, the occurrence of new magic numbers, due to sub-shell gap enhancement or level inversion, becomes an intriguing possibility [4].

The knowledge of atomic masses [9] allows the calculation of nuclear binding (or separation) energies. These quantities have typical systematics, the departure from which indicates the effects of nuclear-structure phenomena, such as shell closures and collectivity. The $Z = 28$ and $N = 50$ shell closures provide a very good nuclear structure testing ground, where many observables, including nuclear masses, remain to be measured.

The ISOLTRAP Penning-trap mass spectrometer has already successfully measured the masses of neutron-rich Ga (up to mass $A = 78$), Cu (up to mass $A = 76$), and Ni (up to mass $A = 69$) isotopes, with precision providing information relevant for the strength of the $N = 40$ sub-shell closure [10]. A very recent measurement of the mass of ^{82}Zn at ISOLTRAP brings the known $N = 50$ empirical shell gap one nucleon closer to the double shell closure at ^{78}Ni. We are now proposing to measure the masses of neutron-rich $^{76-79}$Cu isotopes, for improving the knowledge on the evolution of the $N = 50$ and $Z = 28$ shells towards the doubly magic ^{78}Ni. This information is complementary to the expected results of the accepted proposal INTC-P-316 [11], which represents a laser-spectroscopy study of neutron-rich Cu isotopes with the CRIS setup.

2. Physics motivation

During the last 35 years, the evolution of nuclear shells with the variation of proton and neutron numbers has been the subject of intense study by complementary experimental

methods (for a comprehensive review, see [4]). The crossing of a neutron shell closure, for example, manifests as a sudden decrease, with the addition of one or two extra neutrons, of the two-neutron separation energy, $S_{2n}(Z, N)$. This decrease is quantified by the so-called empirical neutron-shell gap [3]:

$$\Delta_n (Z, N) = S_{2n} (Z, N) - S_{2n} (Z, N + 2), \quad (1)$$

which can be regarded as a measure of the magicity of the nucleus with Z protons and N neutrons.

As a first landmark, the $N = 20$ shell came into attention with the discovery of the "island of inversion" [12], showing no clear decrease with the removal of protons towards $Z = 14$ (Si) [13] and a sudden weakening for $Z < 14$. This evolution is reflected in the systematics of 2^+ excited-state energies and $B(E2; 0^+ \rightarrow 2^+)$ values, shown in Figs. 1(a) and 1(b) (values are taken from [14-16]). It is also supported by the systematics of the $N = 20$ empirical shell gap, Δ_n, presented in Fig. 2(a) [9], where the comparison to the predictions of some theoretical models is also given [7, 17-24].

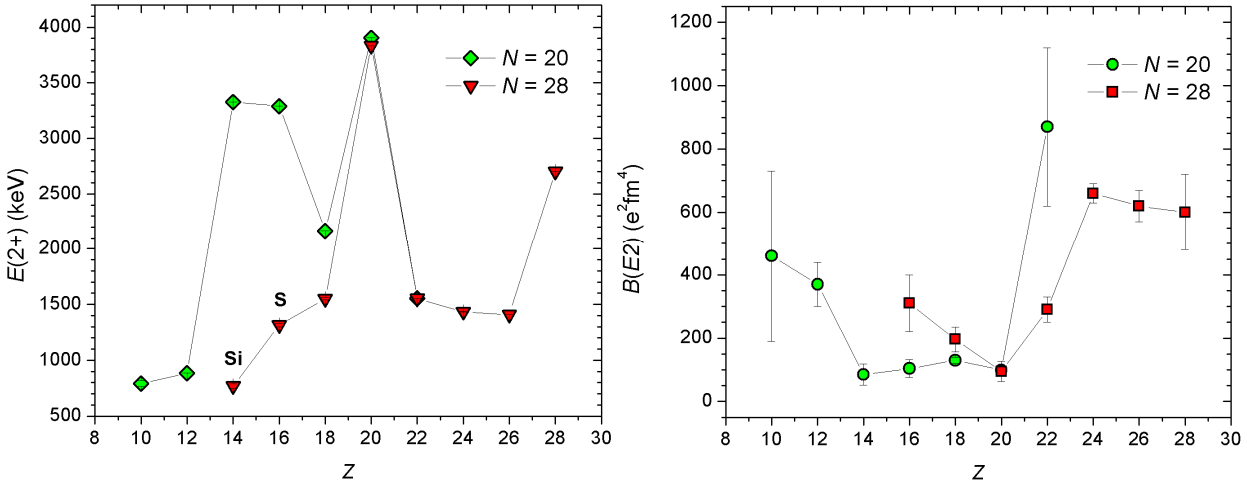

(a) (b)

Figure 1 – Energy of the first 2^+ excited state (a) and $B(E2;0^+ \rightarrow 2^+)$ value (b) for the $N = 20$ and $N = 28$ isotones. The exceptionally high E(2+) values for $Z = 20$ are due to the enhanced magicity of doubly magic nuclei. The values are taken from [14-16]

The weakening of the $N = 28$ shell closure in neutron-rich isotopes is suggested by measurements of the $E(2^+)$ energies in the ^{44}S [15] and ^{42}Si [16] isotopes, which are found to have values considerably lower than the same quantity in the doubly magic ^{48}Ca. The two points are highlighted in Fig. 1(a). For $N = 28$, the known empirical shell gap values, presented in Fig. 2(b), must be completed with additional measurements, in order to confirm the decreasing trend, suggested by the high-uncertainty Cl ($Z = 17$) measurement.

The increase of the empirical shell gap for $N = Z$ nuclei, known under the name of the Wigner effect [3], is apparent in the plots of Fig. 2. The enhanced magicity due to the crossing of the magic proton number $Z = 20$ is also clearly visible in the $N = 28$ plot. It is worth mentioning at this point the relatively good agreement of some of the theoretical calculations with the values of the empirical shell gap, contrasting with the very different predictions the models give outside the experimentally known region.

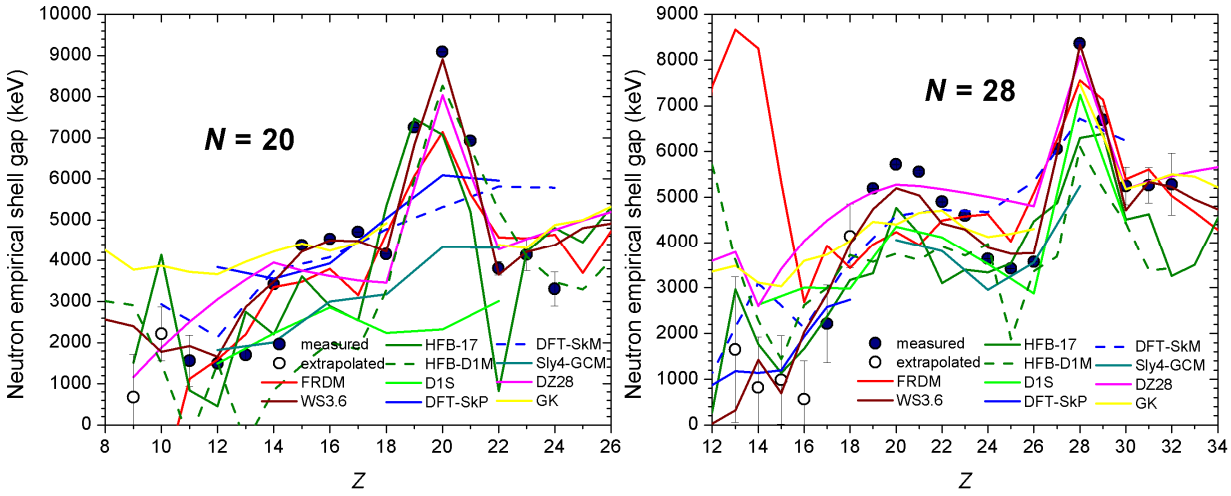

Figure 2 – Empirical shell gap [9] for the $N = 20$ (a) and $N = 28$ (b) isotones and comparison to theoretical predictions [7, 18-24]. The Wigner effect ($Z = N$ in both plots) and the enhanced magicity ($Z = 20$ for the $N = 28$ plot) are visible

The experimental data on the $N = 50$ neutron shell closure suggests a higher robustness with the decrease of the proton number than for the case of $N = 20$ and $N = 28$. The question thus arises whether the so-called "shell quenching" is a phenomenon that characterizes mostly the evolution of the magic numbers up to 28, or it is a universal trend across the entire nuclear chart. The systematics of 2^+ excited-state energies, known down to Zn ($Z = 30$) [14, 25, 26], persists at a value above 1 MeV and even shows an enhancement for ^{80}Zn, as can be seen in Fig. 3(a). The $B(E2; 0^+ \rightarrow 2^+)$ values, presented in Fig. 3(b), show a sudden decrease for the same ^{80}Zn. The available empirical shell gaps [9], known also down to Zn after a recent measurement from ISOLTRAP and plotted in Fig. 4(b), exhibit however a clear reduction towards the doubly magic ^{78}Ni from 6 MeV ($Z = 39$) to 3 MeV ($Z = 30$). The shell-model calculations also require a high effective charge for well reproducing the $B(E2)$ values, suggesting a strong polarization of the $Z = 28$ core [25].

The current theoretical view on the weakening of the $N = 20$ and $N = 28$ shell closures describes it as an effect of the proton-neutron interaction [4-6], as protons are removed from the $Z = 20$ core, leading to a change of the effective single-particle energies. This change reduces the size of the shell gaps and favours collective excitations across the normally inert cores. On the one hand, in the case of $N = 20$, the reduction of the energy gap between the $vf_{7/2}$ and $vd_{3/2}$ orbitals allows the occupation of the *pf* "intruder" neutron orbits. On the other hand, the rapid weakening of the $N = 28$ shell closure is seen as the consequence of the simultaneous reduction of the $Z = 16$ sub-shell and $N = 28$ shell gaps, the former favouring the development of quadrupole collectivity [16]. For a schematic view of the shell-model single-particle energy levels, see Fig. 4(a).

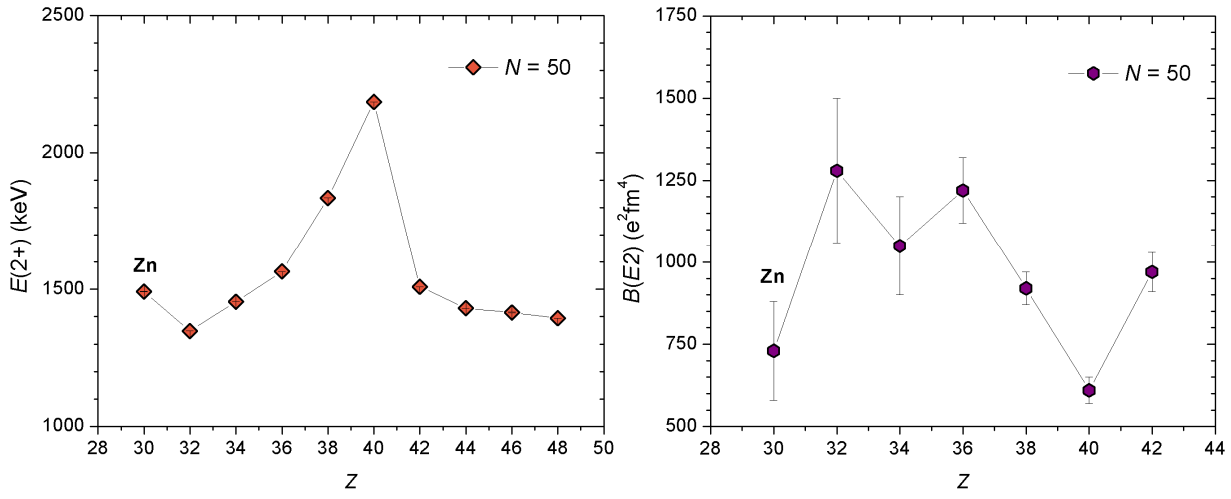

Figure 3 – Energy of the first 2^+ excited state (a) and $B(E2; 0^+ \rightarrow 2^+)$ value (b) for the $N = 50$ isotones. The data are taken from [14, 25, 26]

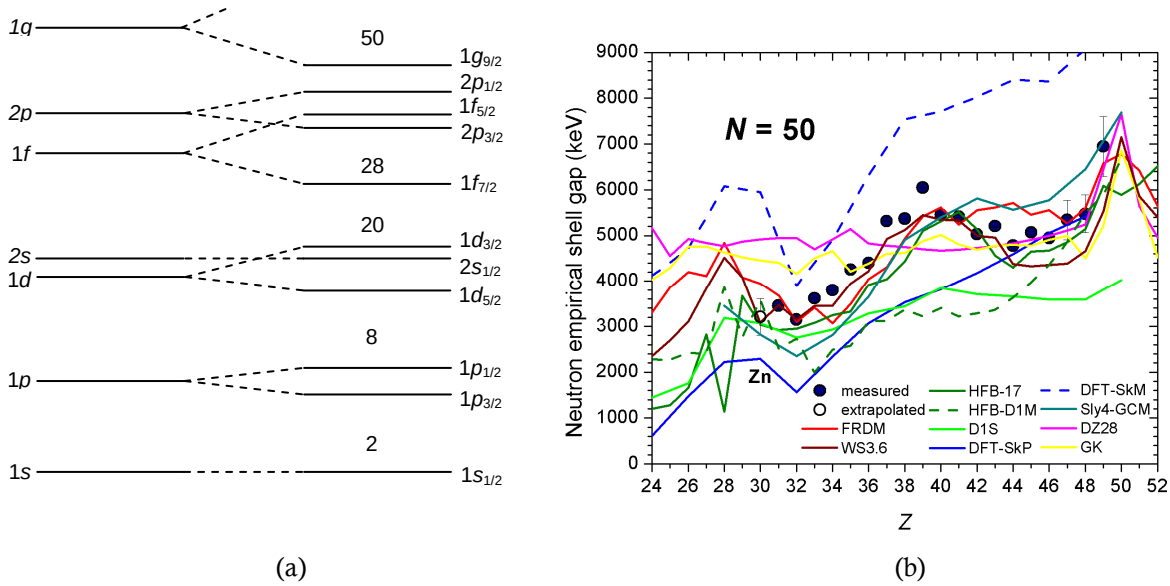

Figure 4 – (a) Schematic of the shell-model single-particle levels (left row). The link to the harmonic-oscillator levels (left row) by the spin-orbit splitting is indicated using the dashed lines; (b) Empirical shell gap [9] for the $N = 50$ isotones and comparison to theoretical predictions [7, 18-24]

The final test of the rigidity of the $N = 50$ shell closure would thus have to come from experimental data on isotopes with $Z < 28$, i.e. after starting to remove protons from the $Z = 28$ core. These isotopes are in many cases prohibitively short lived and not reachable by the current radioactive ion beam production techniques. In the effort to achieve this long term purpose, measurements approaching the doubly magic ^{78}Ni could already offer valuable hints for the $N = 50$ shell evolution below $Z = 28$ and help test the predictions of the different theoretical models in this region of the nuclear chart. This is especially important, since the evolution of the $N = 50$ shell for $Z < 28$ follows very different scenarios depending on the used theoretical model, even when these models reproduce comparably well the already known experimental observables. This is apparent from the plot of the

$N = 50$ empirical shell gap in Fig. 4(b) [9], together with the results of some theoretical calculations [7, 17-24].

An important feature emerging in the plot of the $N = 50$ empirical shell gap is the phenomenon of enhanced magicity at the crossing of the $Z = 28$ closure. The microscopic-macroscopic FRDM [17] and WS3.6 [18] calculations, exhibiting a significant enhancement of the empirical shell gap at $Z = 28$, predict a robust $N = 50$ shell for $Z < 28$. Mean-field approaches such as HFB-17 [19] and HFB-D1M [20], using improved Skyrme and Gogny parameterizations of the nuclear potential, show a much less significant empirical shell gap enhancement and predict a rapid quenching of the $N = 50$ shell for $Z < 28$.

This suggests that probing the strength of the $Z = 28$ closure with the increase of the neutron number could reveal early signs of the $N = 50$ shell evolution when removing protons from the $Z = 28$ core. Already, available experimental data on the $Z = 28$ shell, coming mainly from experiments on Ni, Cu and Zn isotopes, indicate that the filling of the $\nu g_{9/2}$ neutron orbital has a significant impact on the proton structure above and within the $Z = 28$ core. Spectroscopy experiments on Ni isotopes show a decrease of the $E(2^+)$ energy by 330 keV from $N = 42$ to $N = 48$, regarded as a sign of enhanced collectivity [27]. Laser spectroscopy experiments at ISOLDE on Cu isotopes report an inversion of the proton orbitals $\pi p_{3/2}$ and $\pi f_{5/2}$ in ^{75}Cu, interpreted as an effect of the tensor component of the residual proton-neutron interaction [28].

The two-neutron separation energies in the Cu chain between the $N = 40$ and $N = 50$ closures do not follow the typical (almost) linear decrease with the addition of neutrons, as in the case of Se, suggesting that extra binding is gained from collective effects. In Fig. 5(a), the two-neutron separation energies are plotted for nuclei in this region of the nuclear chart. The masses of the Cu isotopes with $N = 48$-50 from the latest Atomic Mass Evaluation [9], ^{77,78}Cu evaluated with an uncertainty of 500 keV and ^{79}Cu only extrapolated, predict that this particular behaviour continues up to the complete filling of the $N = 50$ shell. This is in partial agreement with the results of mean-field calculations such as the recent HFB-D1M functional [20], plotted in Fig. 5(b), which show an increase of the quadrupole deformation around ^{78}Ni, but still predict almost spherical nuclei along the $Z = 28$ and $N = 50$ lines.

The high-precision measurement of the $^{76\text{-}79}$Cu masses would help to clarify the impact of collective correlations right above the doubly magic ^{78}Ni. It would also provide information on the one-particle (proton or neutron) separation energies above $Z = 28$ and below $N = 50$, which can be used, similarly to the two-particle separation energies, for estimating the size of the shell gaps, as the difference in binding between the first proton (neutron) above and the last proton (neutron) below the shell closure. The extrapolated value of the $Z = 28$ gap at $N = 50$, based on the currently known atomic masses, is 3.5 MeV, compared to 6 MeV at N = 40 [4]. A similar extrapolation for the $N = 50$ gap at $Z = 28$ gives a rough estimate of 3 MeV, which is in agreement with Fig. 4. These values are low enough to allow core polarization and excitations across the $Z = 28$ and $N = 50$ gaps for nuclei around the doubly magic ^{78}Ni and for ^{78}Ni itself. Measurements of the masses of Cu isotopes up to the $N = 50$ closure would help to improve the precision of these estimates, as well as the accuracy of theoretical predictions, and shed light on the seemingly magic character of ^{78}Ni.

Decay spectroscopy measurements report the existence of a 1.27 s half-life isomer in ^{76}Cu [29], which however was not confirmed by other experimental studies, such as the one in [30]. The excitation energy of the isomer is extrapolated to 0 keV in the latest Atomic Mass Evaluation [9], with an uncertainty of 200 keV, while the assignment to the ground state or

excited state is also uncertain. The high-resolution Penning trap of the ISOLTRAP experiment was successfully used for resolving two isomers and the ground state of ^{70}Cu, thus unambiguously providing, together with decay-spectroscopy studies, its low-energy level scheme [31]. A measurement of the mass of the ^{76}Cu isomer would offer direct evidence for its existence, independently of its decay properties.

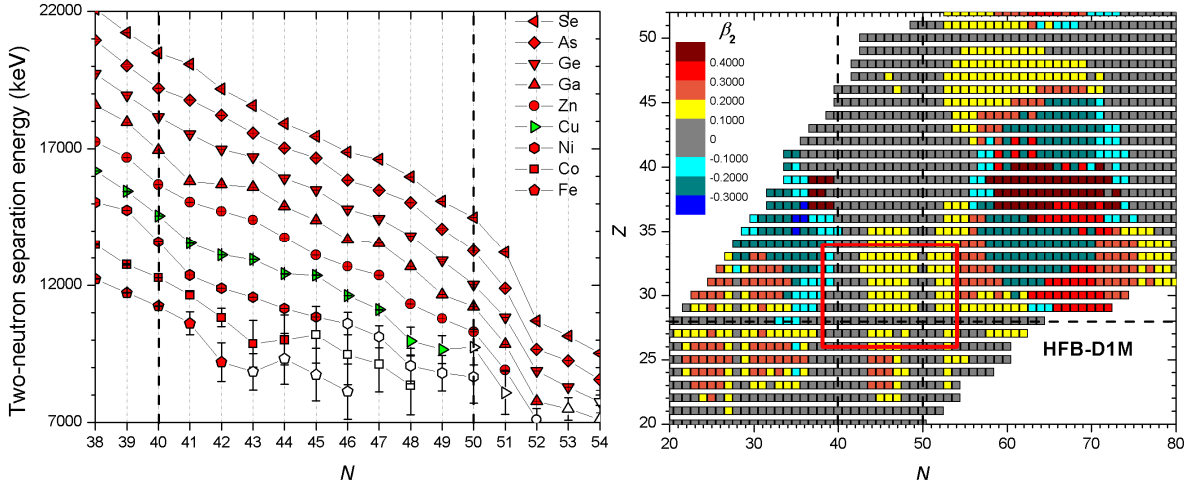

Figure 5 – Two-neutron separation energies around the Ni chain [9] (a) and HFB-D1M predictions of the quadrupole deformation (b) [20]. The red frame in the right plot marks the area corresponding to the left plot

3. Experimental setup

The ISOLTRAP Penning-trap mass spectrometer has been an integral part of the ISOLDE on-line experiments for more than two decades. It now comprises four traps (three for preparation, one for measurement), combining different experimental techniques in order to provide high-precision mass measurements on radioactive isotopes from the ISOLDE facility. A full list of the ISOLTRAP measurements and publications can be found on the experiment webpage [32], while a part of the more recent results is reviewed in [33].

The mass measurements are performed by the time-of-flight ion-cyclotron resonance technique, using a hyperbolic Penning trap ("precision Penning trap" in Fig. 6) [34, 35]. This technique requires an isobaric-pure beam of narrow energy distribution and low transversal emittance. For this purpose, the ISOLDE 30-60 keV beam is decelerated in front of a gas-filled linear radiofrequency quadrupole [36] ("RFQ cooler and buncher" in Fig. 6), which accumulates and cools the energetic quasi-continuous ion beam from the ISOLDE facility and ejects thermalized, short ion bunches with about 3 keV kinetic energy. The bunch energy is further reduced to a few tens of eV before the ions enter the cylindrical gas-filled Penning trap ("preparation Penning trap" in Fig. 6). Its purpose is not only to match the energy distribution of the ion bunch to the requirements of the precision trap, but also to perform a suppression of the contaminant species in the ion ensemble, by mass-selective resonant buffer-gas cooling [37]. A detailed description of the ISOLTRAP experiment is given in the review paper [38].

A recent addition to the setup is a multi-reflection time-of-flight (MR-TOF) mass separator ("MR-TOF mass separator" in Fig. 6), commissioned in 2010 and already successfully used

during the 2011 experimental campaign [39]. The device is designed to increase the isobaric purity of the ISOLDE beam by performing a time-of-flight separation of the different beam components (ion of interest and contaminants), enough for a clear-cut selection to be possible with a fast-switching Brandbury-Nielsen ion gate ("BN beam gate" in Fig. 6). In comparison to the gas-filled Penning trap, this device requires an order of magnitude less trapping time (only tens of milliseconds) in order to achieve the same resolving power, thus allowing to access shorter-lived ion species. The possibility of calibrating this device for direct mass measurements of very short half-life isotopes is currently under investigation and is already part of an accepted ISOLTRAP proposal INTC-P-317 [40].

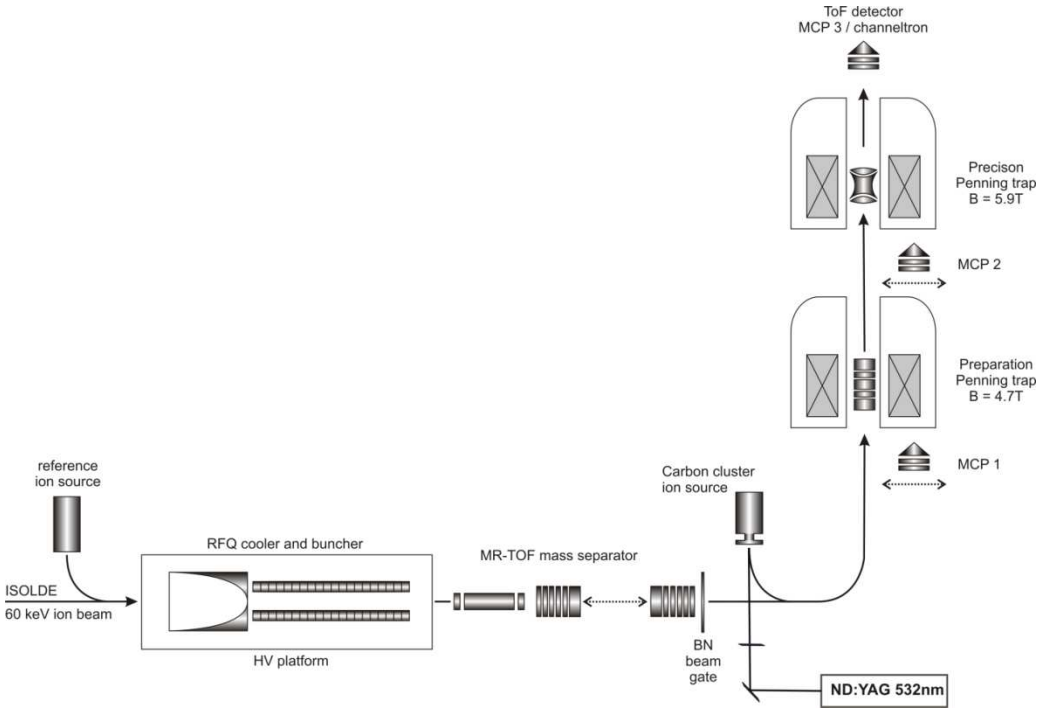

Figure 6 – Schematic of the ISOLTRAP setup. For details see text

The ISOLTRAP setup has been used so far for measuring the mass of ions with yields as low as 10^2 ions/μC and half-lives as short as tens of milliseconds (the lowest half-life of an ion measured so far is 63 ms [41]). A suppression of the contaminant species of four orders of magnitude can be achieved. The contaminant resolving power of the gas-filled Penning trap is typically of the order of 5×10^4, while the MR-TOF can reach resolving powers above 10^5 even for short-lived species. A new technique has been implemented at ISOLTRAP, consisting of multiple injections in the gas-filled Penning trap of ion bunches which have been previously separated with the MR-TOF. This technique improves the ion-of-interest count-rate in the precision Penning-trap when dealing with low yields of long-lived species and also increases the maximum contamination ratio that can be suppressed.

The mass resolving power of the measurement Penning trap, determined by the width of the time-of-flight ion-cyclotron resonance curve, depends on the ion mass and on the time the ion motion is excited inside the trap. More specifically, for ^{76}Cu and a 1.5 s excitation time, the FWHM of the resonance curve is, in units of energy, roughly 50 keV (scaling inversely with the excitation time). The quoted half-life of the ^{76m}Cu isomer (1.27 s) allows exciting

the ion motion for 3 s without a too large drop in ion count due to decay. This means that the ^{76m}Cu isomer can be resolved from the ground state, if the yields of the two states are comparable and the energy difference is above 25 keV.

4. Beam time requests

The detailed beam time requests are presented in Table 1. We point out that, even if the masses of the ^{77,78}Cu isotopes appear as measured, their values were determined as a by-product of a non-dedicated setup, with a technique that was not fully optimized for mass measurements [42]. These values must be confronted with the results of a high-precision mass measurement, such as the one provided by the ISOLTRAP setup, before the newly proposed technique can be fully validated.

Cu isotopes up to mass 76 (except the ^{76m}Cu isomer) have been successfully studied at ISOLTRAP, in an experiment in which protons were shot onto a UC_x target and ionised using RILIS [10]. The proposed Cu isotopes, except for ^{79}Cu, have been produced at ISOLDE for decay and laser-spectroscopy experiments (e.g. [30, 43]). No additional target development would be required for this proposal. The yields in Table 1 are taken from the ISOLDE database and have been confirmed, up to ^{78}Cu, during the runs quoted in [30]. The yield for the isotope ^{79}Cu is an extrapolated value [44].

The major contaminating isobars of the requested Cu beams are the Rb and Ga isotopes. Shooting protons onto a neutron converter would greatly suppress the Rb contamination. Based on measurements from [45], we can expect a suppression of the Rb yield down to 10^5 ions/μC on mass 80, (which would be naturally further reduced towards mass 76 due to the very neutron- deficient character) and of the Ga yield to around 10^5 ions/μC on all masses of interest.

Table 1

Isotope	Half-life (s)	Mass uncertainty (keV)	Target	Yield† (ions/μC)	Ion source	Shifts
^{76m}Cu	1.27(30)	extrapolated	UC_x	$2\times10^{4*}$	RILIS	2
^{77}Cu	0.469(8)	500		2×10^{3}		2
^{78}Cu	0.342(11)	500		2×10^{2}		3
^{79}Cu	0.188(25)	extrapolated		20		6
Yield optimization with the HRS						1
TOTAL						**14**

† *Values for protons shot directly on the target.*

* *Yield data makes no reference to the nucleus being in the isomeric state.*

The resolving power required for separating the Rb and Ga isobars is around and below 4×10^3. A further suppression of the contaminating ions can thus be achieved by taking the beam through the High Resolution Separator (HRS) of ISOLDE and by using the separator slits. The efficiency of the HRS in separating a neutron-rich isotope from lighter surface ionized isobars has been successfully tested in the reduction of the Na contamination from a Mg beam. A factor 2 suppression of the Ga contamination can be expected by using the HRS [46], without affecting the Cu-beam intensity. The target and line temperatures can also significantly influence the Ga yield, a reduction of up to a factor 5 being possible by

finding optimal working conditions [44]. An extra shift is thus required, apart from the ones for the mass measurement program, dedicated to the optimization of ion production and transport through the HRS for the reduction of the beam contamination.

Summary of requested shifts: In total, a number of 14 shifts are requested, 13 for the actual mass measurements and 1 for the reduction of the beam contamination by tuning the target and line temperatures and by optimizing the HRS.

References:

[1] M. G. Mayer, Phys. Rev. **75**, 1969-1970 (1949).
[2] O. Haxel, J. H. D. Jensen, H. E. Suess, Phys. Rev. **75**, 1766–1766 (1949).
[3] D. Lunney, J. M. Pearson, C. Thibault, Rev. Mod. Phys. **75**, 1021-1082 (2003).
[4] O. Sorlin, M.-G. Porquet, Progr. Part. Nucl. Phys. **61**, 602-673 (2008).
[5] T. Otsuka et al., Phys. Rev. Lett. **87**, 082502-1-4 (2001).
[6] T. Otsuka, D.Abe, Progr. Part. Nucl. Phys. **59**, 425-431 (2007).
[7] M. Bender, G. F. Bertsch, P.-H. Heenen, Phys. Rev. Lett. **94**, 102503-1-4 (2005).
[8] M. Bender, G. F. Bertsch, P.-H. Heenen, Phys. Rev. C **78**, 054312-1-7 (2008).
[9] G. Audi, W. Meng, Private Communication, April 2011.
[10] C. Guénaut et al., Phys. Rev. C **75**, 044303-1-12 (2007).
[11] G. Neyens et al., proposal INTC-2011-052 (2011).
[12] C. Thibault et al., Phys. Rev. C **12**, 644-657 (1975).
[13] R. W. Ibbotson et al., Phys. Rev. Lett. **80**, 2081-2084 (1998).
[14] S. Raman, C. W. Nestor, Jr., P. Tikkanen, At. Data Nucl. Data. Tables **78**, 1-128 (2001).
[15] T. Glasmacher et al., Phys. Lett. B **395**, 163-168 (1997).
[16] B. Bastin et al., Phys. Rev. Lett **99**, 022503-1-4 (2007).
[17] P. Moller, J. R. Nix, W. D. Myers, W. J. Swiatecki, At. Data and Nucl. Data Tables **59**, 185-383 (1995).
[18] M. Liu, N. Wang, Y. Deng, X. Wu, Phys. Rev. C **84**, 014333-1-8 (2011).
[19] S. Goriely, N. Chamel, J. M. Pearson, Phys. Rev. Lett. **102**, 152503-1-4 (2009).
[20] S. Goriely, S. Hilaire, M. Girod, S. Péru, Phys. Rev. Lett. **102,** 242501-1-4 (2009).
[21] J. -P. Delaroche et al., Phys. Rev. C **81**, 014303-1-23 (2010).
[22] M.V. Stoitsov et al., Phys. Rev. C **68**, 054312-1-11 (2003).
[23] J. Duflo, A. P. Zuker, Phys. Rev. C **52**, R23–R27 (1995).
[24] E. Comay, I. Kelson, A. Zidon, At. Data Nucl. Data Tables **39**, 235-240 (1988).
[25] J. van de Walle et al., Phys. Rev. Lett **99**, 142501-1-4 (2007).
[26] A. Gade et al., Phys. Rev. C **81**, 064326-1-7 (2010).
[27] F. Azaiez, AIP. Conf. Proc. **802**, 95-102 (2005).
[28] K. T. Flanagan et al., Phys. Rev. Lett. **103**, 142501-1-4 (2009).

[29] J. A. Winger et al., Phys. Rev. C **42**, 954–960 (1990).
[30] J. Van Roosbroeck et al., Phys. Rev. C **71**, 054307-1-19 (2005).
[31] J. Van Roosbroeck et al., Phys. Rev. Lett. **92**, 112501-1-4 (2004).
[32] ISOLTRAP webpage: www.cern.ch/isoltrap.
[33] M. Kowalska for the ISOLTRAP collaboration, "ISOLTRAP results 2006-2009," Hyperfine Interact. **196**, 199-203 (2010).
[34] G. Bollen, R. B. Moore, G. Savard, H. Stolzenberg, J. Appl. Phys. **68**, 4355-4374 (1990).
[35] M. König et al., Int. J. Mass. Spectrom. Ion Processes **142**, 95-116 (1995).
[36] F. Herfurth et al., Nucl. Instrum. Meth. A **469**, 254-275 (2001).
[37] G. Savard et al., Phys. Lett. A **158**, 247-252 (1990).
[38] M. Mukherjee et al., Eur. Phys. J. A **35**, 1-29 (2008).
[39] R. N. Wolf, M. Eritt, G. Marx, L. Schweikhard, Hyperfine Interact. **199**, 115-122 (2011); R. N. Wolf, G. Marx, M. Rosenbusch, L. Schweikhard, Int. J. Mass Spectrom., in press, doi:10.1016/j.ijms.2011.12.006.
[40] S. Kreim et al., proposal INTC-P-317 (2011).
[41] S. Naimi et al., Phys. Rev. Lett **105**, 032502-1-4 (2010).
[42] P. A. Hausladen et al., Int. J. Mass Spectrom. **251**, 119-124 (2009).
[43] U. Köster et al., Phys. Rev. C **84**, 034320-1-7 (2011).
[44] Th. Stora, Private Communication (2011).
[45] U. Köster et al., AIP Conf. Proc. **798**, 315-323 (2005).
[46] T. J. Giles, Private Communication (2011).

Appendix

DESCRIPTION OF THE PROPOSED EXPERIMENT

The experimental setup comprises: ISOLDE central beam line and ISOLTRAP setup. The preliminary safety file is the document “safety-requirements-ISOLDE-ISOLTRAP" with the corresponding attached documents dealing with the different hazards: acetone, cadmium, ethanol, helium, isopropanol, nitrogen, and noise. Furthermore, the existing ISIEC file “ISIEC_ISOLTRAP_2010-11-18” is also part of the safety documents made available for the ISOLTRAP experiment.

Part of the	Availability	Design and manufacturing
ISOLTRAP setup	☒ Existing	☒ To be used without any modification

HAZARDS GENERATED BY THE EXPERIMENT

Hazards named in the document relevant for the fixed ISOLTRAP installation.